NASA TM-77962

NASA TECHNICAL MEMORANDUM NASA TM-77962

NASA-TM-77962 19860012045

# THREE-DIMENSIONAL BOUNDARY LAYER ANALYSIS PROGRAM "BLAY" AND ITS APPLICATION

Ken-ichi Matsuno and Tomiko Ishiguro

Translation of Proceedings of the NAL Symposium on Aircraft Computational Aerodynamics, Tokyo, Japan, June 30 - July 1, 1983, pages 207-218



NATIONAL AERONAUTICS AND SPACE ADMINISTRATION
WASHINGTON D.C. 20546 JANUARY 1986

STANDARD TITLE PAGE

| 1. Report No. NASA TM-77962 | 2. Government Accession No. | 3. Recipient's Catalog No. |
|---|---|---|
| 4. Title and Subtitle THREE-DIMENSIONAL BOUNDARY LAYER ANALYSIS PROGRAM "BLAY" AND ITS APPLICATION | | 5. Report Date January, 1986 |
| | | 6. Performing Organization Code |
| 7. Author(s) Ken-ichi Matsuno and Tomiko Ishiguro | | 8. Performing Organization Report No. |
| | | 10. Work Unit No. |
| 9. Performing Organization Name and Address SCITRAN Box 5456 Santa Barbara, CA 93108 | | 11. Contract or Grant No. NASw- 4004 |
| | | 13. Type of Report and Period Covered Translation |
| 12. Sponsoring Agency Name and Address National Aeronautics and Space Administration Washington, D.C. 20546 | | 14. Sponsoring Agency Code |

15. Supplementary Notes

Translation of Proceedings of the NAL Symposium on Aircraft Computational Aerodynamics, Tokyo, Japan, June 30 - July 1, 1983, pages 207-218 (85N26632).

16. Abstract

The boundary layer calculation program (BLAY) is a program code which accurately analyzes the three-dimensional boundary layer of a wing with an undefined plane. In comparison with other preexisting programs, the BLAY is characterized by the following (1) the time required for computation is shorter than any other; (2) the program is adaptable to a parallel processing computer, and (3) the program is associated with a secondary accuracy in the z-direction. As a boundary layer modification to transonic nonviscous flow analysis programs, it is used to adjust viscous and nonviscous interference problems repeatedly. Its efficiency is an important factor in cost reduction in aircraft designing.

| 17. Key Words (Selected by Author(s)) | | 18. Distribution Statement Unclassified and Unlimited | |
|---|---|---|---|
| 19. Security Classif. (of this report) Unclassified | 20. Security Classif. (of this page) Unclassified | 21. No. of Pages 24 | 22. Price |



N85-26632-ORIGINAL
N86-21516#
N-155,846

# THREE-DIMENSIONAL BOUNDARY LAYER ANALYSIS PROGRAM "BLAY" AND ITS APPLICATION

*/207

Ken-ichi Matsuno and Tomiko Ishiguro

## 1. Introduction

Among the important elements in the transonic aerodynamic design of a wing is the evaluation of viscous strength. The flow field of the transonic region itself is an aerodynamically critical region. For example, even when considering only the shock wave on the wing surface, it is a well known fact that the shock position and shock strength differ significantly when comparing the calculated results for the case where non-viscous flow is assumed and where viscous effects are taken into account. The viscous effects for adhesive flow under flight cruise conditions can be evaluated with sufficient accuracy even by applying boundary layer equations. Therefore, the computational aerodynamic technique currently being utilized in aerodynamic design involves the method of compensating in the transonic total potential flow analysis program by incorporating the boundary layer effects. This method is more realistic than considering developmental factors such as computing costs and the computer hard level calculation method. Thus, a variety of test runs are currently being conducted.

The BLAY (boundary layer calculation program) is the acronym for a program that analyzes rigorously the three-dimensional boundary layer of a wing having an arbitrary planar configuration. It is based on a research program developed in the 1979-1980 period which subsequently was further developed into a general purpose

---

* Numbers in margin indicate pagination of foreign text.

program with the objective of its conversion into a production code.

The purpose of this paper is to present a general survey of the development status among several nations in their three-dimensional boundary layer analysis programs dealing with wing configurations; to discuss the characteristics of the BLAY program in a comparative evaluation against those programs; and to point out that, among all presently existing computation programs, the BLAY is outstanding in many factors including computation efficiency. As examples of computations employing the BLAY, we will introduce the results on some wing configurations of recent interest, including the forward swept wing.

## 2. Three-dimensional boundary layer analysis program on a wing

Since we are here particularly interested in solving rigorously the boundary layer equation(s), the so-called integration method, based on Karman's integration equation, will be omitted from consideration on the ground that it is an approximation analysis method. The three-dimensional boundary layer analysis program which addresses wing configurations is being developed energetically in particular by airframe manufacturers in the United States, and by the national aeronautical research laboratories in Europe, as can be deduced from the news on those subject areas. These were reported continously in the 1977-1979 period as shown in Table 1. This is exactly the time frame during which Jameson's Transonic Total Potential Flow Analysis Program (FLO 22) was published. In our country, too, R&D was initiated in 1978 at the Aero Tech Lab (Ko Gi Ken) and followed the course shown in Table 1, and produced the current program, BLAY.

### 2.1 Coordinate system structure and boundary layer equations

In the case of computational programs of this type, which are evaluated against computation criteria for a real (finite) wing, the coordinate system to be used may constrain the applicable scope of the program on the region within which the computation can be performed. Figure 1 compares the coordinate system employed in several computation programs and the BLAY system. The coordinate system used by Nash and Scruggs, and others [2,10] is a polar coordinate system (r, θ, y) applicable to the straight line portion of a tapered wing and cannot be applied to parts with strakes or kinks. In MacLean's [4] coordinate system, a cross flow coordinate system is created from the leading edge stagnation line and can thereby be applied to various wing configurations, but has the following defects: generally, there occurs a region on the wing tip(s) where computation is impossible; it is difficult to establish initial conditions at the wing root; the computation points at the wing root differ at all coordinate lines and processing becomes complex; the non-viscous data necessary as a boundary condition are generally given at fixed per cent chord, and fixed per cent span. Therefore, there is no match with the coordinate points of the boundary layer computation, and it becomes necessary to employ a complicated interpolation routine; /20

TABLE 1. Three-dimensional boundary layer analysis programs for wings (references 1 through 13)

Boundary Layer Methods for Finite Wings

| | | | |
|---|---|---|---|
| United States | | | |
| Lockheed Corp. | Nash and Scruggs | (1972) | Explicit Scheme |
| | Nash and Scruggs | (1978) | Implicit Scheme |
| McDonnel Douglas Corp. | Cebeci, Kaups and Ramsey | (1977) | Regular Box Scheme |
| | | (1978) | Modification of a scheme |
| | | \| | Zig-zag Box Scheme |
| | | (1979) | Characteristic Box Scheme |
| Boeing Co. | McLean | (1977) | Implicit Scheme |
| | McLean and Randall | (1978) | Pilot code |
| Europe | | | |
| Britain | Bradshaw, Mizner and Unsworth | (1975) | for straigt tapered wings |
| Netherlands | Lindhout and De Boer | (1976) | for laminar flows |
| | Lindhout et al. | (1979) | for turbulent flows |
| West Germany | Kordulla | (1977) | Krause Zig-zag Scheme |
| | Rostgi and Rodi | (1979) | for straight tapered wings |
| Japan NAL | (1978 : start) | | |
| | (1979) | Research code ; for rectangular wings | |
| | | Presentation of a new scheme ( PC-CN Scheme ) | |
| | (1980) | Research code ; for arbitrary finite wings | |
| | (1981) | Modification of the scheme | |
| | (1982) | Development of a pilot code | |
| | (1983) | —— BLAY code | |

similarly, in the case of output, a need arises to redistribute the data on a fixed per cent span. Among the coordinate systems used by Kordulla [9], the coordinates for the systems documented in the cartesian system are normalized in the chord direction at 0 at the leading edge and at 1 (unity) at the trailing edge, and is appropriate for input/output of data at a fixed per cent chord and fixed per cent span. Furthermore, in this coordinate system, the velocity component is taken directly in the direction of the cartesian system.

The coordinate system by Cebeci, et al. [8] uses non-cross flow coordinates that establishes fixed per cent chord and fixed per cent span as coordinates (x,y) initially. In this case, the number of terms appearing in the boundary layer equation is somewhat greater than that for the cross flow system; and is characterized by the fact that the establishment of initial conditions is direct, and, therefore, easy, at the leading edge stagnation line, at the wing root area and at the wing tip area. Also it is suitable for data input/output. This coordinate system and Kordulla's coordinate system can be applied to any arbitrary wing configuration and can be addressed to the entire wing region. From the above comparison, it is seen that the coordinate system used by Cebeci, et al. [8] is the most appropriate for the case of addressing an assumed wing configuration. The BLAY uses this coordinate system.

Using the code indicated at the bottom of Figure 1, the non-cross flow coordinate system is expressed as

$$dl^2 = h_1^2 dx^2 + h_2^2 dz^2 + 2 h_1 h_2 \cos\theta \, dx \, dz + dy^2 \tag{1}$$

and the compressible turbulent flow boundary layer equation is expressed as

continuous equation:

$$\frac{\partial}{\partial x}(\rho u h_2 \sin\theta) + \frac{\partial}{\partial z}(\rho w h_1 \sin\theta) + \frac{\partial}{\partial y}(\overline{\rho v} h_1 h_2 \sin\theta) = 0 \tag{2}$$

x--momentum equation:

$$\frac{\rho u}{h_1}\frac{\partial u}{\partial x}+\frac{\rho w}{h_2}\frac{\partial u}{\partial z}+\overline{\rho v}\frac{\partial u}{\partial y}-\rho u^2 K_1 \cot\theta$$

$$+\rho w^2 K_2 \csc\theta+\rho u w K_{12}=-\frac{\csc^2\theta}{h_1}\frac{\partial P}{\partial x}$$

$$+\frac{\cot\theta\csc\theta}{h_2}\frac{\partial P}{\partial z}+\frac{\partial}{\partial y}\left(\mu\frac{\partial u}{\partial y}-\rho\overline{u'v'}\right) \tag{3}$$

z--momentum equation

$$\frac{\rho u}{h_1}\frac{\partial w}{\partial x}+\frac{\rho w}{h_2}\frac{\partial w}{\partial z}+\overline{\rho v}\frac{\partial w}{\partial y}-\rho w^2 K_2 \cot\theta$$

$$+\rho u^2 K_1 \csc\theta+\rho u w K_{21}=\frac{\cot\theta\csc\theta}{h_1}\frac{\partial P}{\partial x}$$

$$-\frac{\csc^2\theta}{h_2}\frac{\partial p}{\partial z}+\frac{\partial}{\partial y}\left(\mu\frac{\partial w}{\partial y}-\rho\overline{v'w'}\right) \tag{4}$$

/210

Energy equation:

$$\frac{\rho u}{h_1}\frac{\partial H}{\partial x}+\frac{\rho w}{h_2}\frac{\partial H}{\partial z}+\overline{\rho v}\frac{\partial H}{\partial y}=\frac{\partial}{\partial y}\left\{\frac{\mu}{P_r}\frac{\partial H}{\partial y}\right.$$

$$+\mu\left(1-\frac{1}{P_r}\right)\frac{1}{2}\frac{\partial}{\partial y}\left(u^2+w^2+2uw\cos\theta\right) \tag{5}$$

$$\left.-\rho\overline{v'H'}\right\}$$

Here $\overline{\rho v}=\rho v+\overline{\rho' v'}$ ; $\rho$ is density; p is pressure; u,w,v are the velocity components in the x,y,z directions; H is total enthalpy; $\mu$ is the coefficient of viscosity; $P_r$ is the Prandtl number. The geometric parameters $K_1, K_2, K_{12}$ and $K_{21}$ are given by the following equations:

$$K_1=\frac{1}{h_1 h_2 \sin\theta}\left\{\frac{\partial}{\partial x}(h_2\cos\theta)-\frac{\partial h_1}{\partial z}\right\} \tag{6a}$$

$$K_2=\frac{1}{h_1 h_2 \sin\theta}\left\{\frac{\partial}{\partial z}(h_1\cos\theta)-\frac{\partial h_2}{\partial x}\right\} \tag{6b}$$

$$K_{12}=\frac{1}{\sin\theta}\left\{-\left(K_1+\frac{1}{h_1}\frac{\partial\theta}{\partial x}\right)+\cos\theta\left(K_2+\frac{1}{h_2}\frac{\partial\theta}{\partial z}\right)\right\} \tag{6c}$$

$$K_{21}=\frac{1}{\sin\theta}\left\{-\left(K_2+\frac{1}{h_2}\frac{\partial\theta}{\partial z}\right)+\cos\theta\left(K_1+\frac{1}{h_1}\frac{\partial\theta}{\partial x}\right)\right\} \tag{6d}$$

The Reynolds' stress, $\overline{u'v'}$ $\overline{v'w'}$ and $\overline{v'H'}$ appearing in (3) through (5) is evaluated by means of the Cebeci type vortex viscous two-dimensional algebraic model [13].

Boundary conditions are adhesive adiabatic wall conditions at the wing surface:

/209

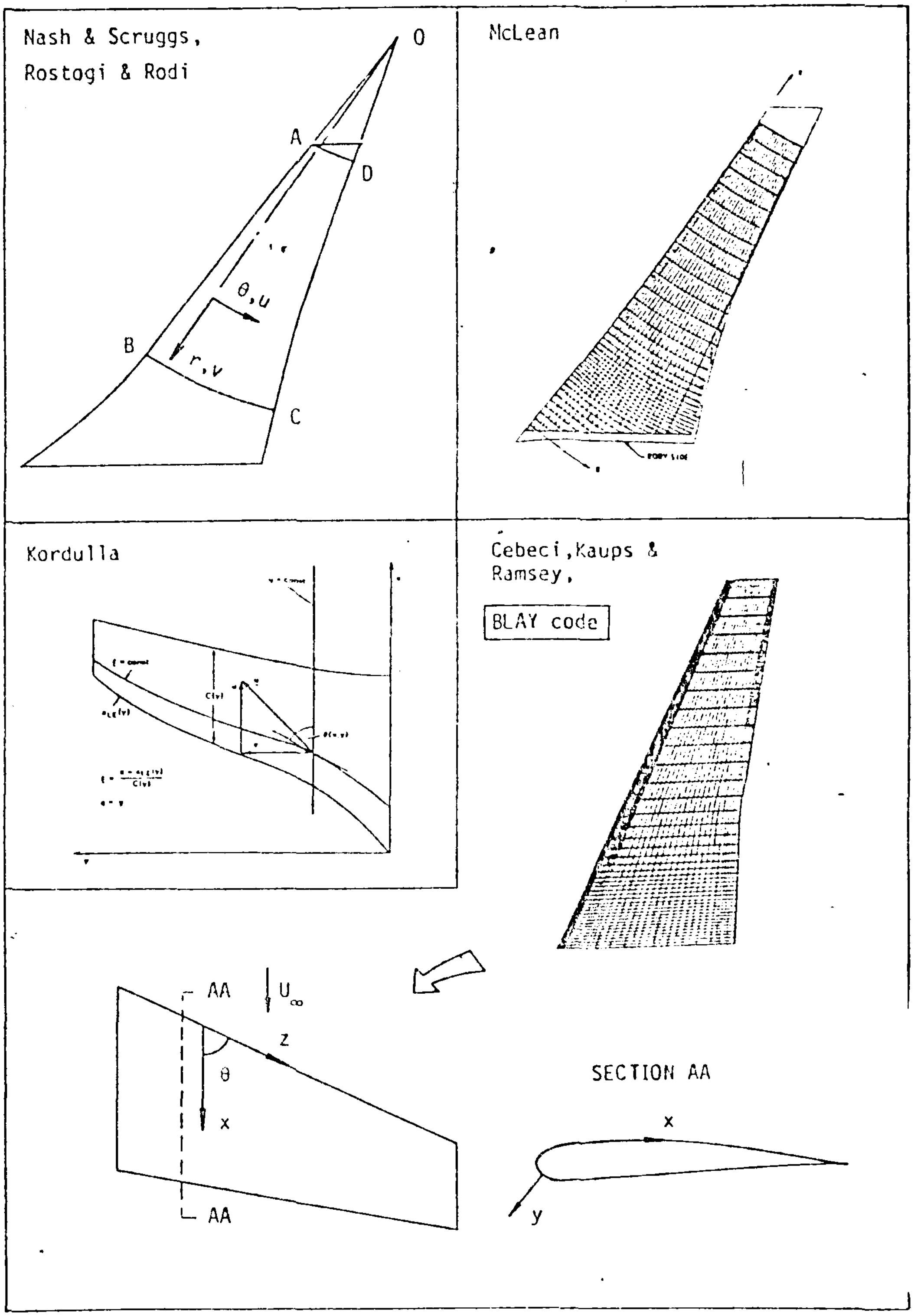


Figure 1. Comparison of various computer program coordinate systems and the BLAY coordinate system.

$$y=0\ ;\ u=w=v=0\ ,\ (\partial H/\partial y)_{wall}=0 \tag{7}$$

The value of the non-viscous flow on the outer fringe of the boundary layer is given by:

$$y=\delta\ ;\ u=u_e(x,z),\ w=w_e(x,z),\ H=H_e \tag{8}$$

The initial conditions must be given by x = 0 (leading edge stagnation line) z = 0 (wing root); or by $z = z_{tip}$ (wing tip). In the case of BLAY, the "stagnation equation" [3] is used at x = 0; the infinite sweep back wing equation [3] by which the z--integral term is set at zero for z = 0 or $z = z_{tip}$. Thereby, the initial respective profiles are calculated.

In the actual calculation, the Cebeci type [3] is converted into equations (2) through (5) and the difference scheme is employed in the boundary layer coordinate system. For the boundary layer conversion, not only can the peculiarity of the equation at x = 0 be eliminated, but in this type three-dimensional laminar flow/turbulent flow region, the boundary layer conversion is effective also from the standpoint of conserving the computer memory capacity and computer line.

## 2.2 Numerical calculation method

The three-dimensional boundary layer equation differs greatly in its character from the two-dimensional boundary layer equation in that the hyperbolic/parabolic forms, which are known as the basic principle of Raetz's zone of influence and zone of dependence, accrue to it. As shown in Figure 2, the disturbance generated at a point P within the boundary layer propagates into the normal line A-B on the body surface, having passed P instantaneously by virtue of its character as a parabolic type. Simultaneously, by virtue of its character as a hyperbolic type, it proceeds downstream along all stream lines passing through the line A-B. Therefore, the disturbance generated at point P is transmitted to the entire wedge (cuneiform) region (the zone of influence) formed by the surface including the outermost streamline passing through the line A-B on the down-

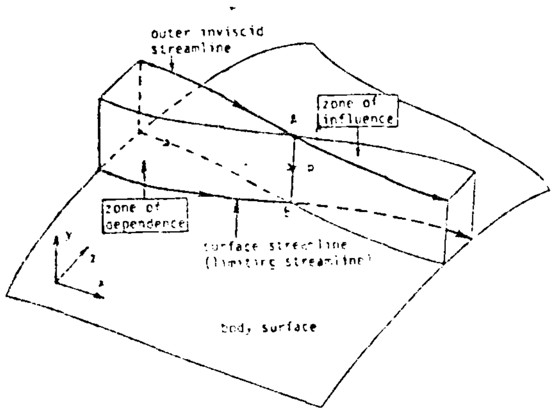


Figure 2. Three-dimensional boundary layer zones of influence and dependence.

stream side. Conversely, the condition at point P is determined by the total reverse wedge region (zone of dependence) surrounded by the surface that includes the outermost stream line(s) passing through the line A-B on the upstream side. Therefore, when calculating the value of point P, it is impossible to perform a stable and reliable calculation unless a difference scheme is applied that will take into account all information on the zone of dependence.

The numerical calculation method can be formulated by a variety of schemes by considering the character of all the above described boundary layer equations and depending on how to perform difference approximation in terms of differentials. The boundary layer equations contain the following differential terms:

$$\frac{\partial(\;)}{\partial x},\ \frac{\partial(\;)}{\partial z},\ \frac{\partial(\;)}{\partial y},\ \frac{\partial}{\partial y}\left(\nu\frac{\partial(\;)}{\partial y}\right) \tag{9}$$

Using the symbols $\square$, 0, +, and x to represent the above mentioned terms diagrammatically, Figure 3 shows the comparison between the various difference schemes and the BLAY shown in Table 1. As to the remarks on the Box method in Figure 3, it is to be noted that since the second order differential terms on y are converted to simultaneous first order differentials, the x symbol does not appear. Considering in general the representative-difference schemes (a) through (e) /211 listed in Figure 3, it is seen that they are characterized by a number of properties as follows: (1) considering the stability of the difference scheme, it is implicit relative to the y direction; however, the interative process is introduced to linearize the non-linear terms and the computer operation load is increased, making the process inefficient [schemes (a) through (e)]; (2) the stability requirements on the numerical calculation dictate the need for a scheme that depends on the direction of flow. In other words, the difference configuration changes in response to the w code [schemes (a), (b), (c), (e)]; (3) being a totally gradual processing algorithm, a parallel processing operation cannot be performed [schemes (b), (c), (d), (e)]; (4) the coordinate width in the z direction changes and when w is less than 0, the accuracy in the z direction deteriorates to the first order of coordinate width [schemes (a) through (e)].

Property (2) described above is generally not suited to parallel processing operation because of the entry of the IF text or the procedure corresponding to it within the computation loop. Also, in the presence of property (3), the parallel processing operation is totally impossible. Calculation aerodynamics is a design tool and the computer to be used in the future will be a super computer for exclusive scientific and technical application which must have a parallel processing operation system as its basis.

The BLAY difference scheme (predictor/corrector type Crank (algebraic)-Nicholson (PC-CN) scheme [11,13]) is a newly developed difference scheme which provides for higher efficiency and higher accuracy as well as being suitable for parallel processing operation by a specialized scientific and technical super computer. We next introduce this system briefly.

The boundary layer equation considers the pressure gradient as functions of x, z whose characteristics are represented by a scalar equation that can be expressed as follows:

$$u\frac{\partial u}{\partial x} + func\left(x, z, u\frac{\partial u}{\partial z}, \frac{\partial u}{\partial y}\right) = \frac{\partial}{\partial y}\left(\nu\frac{\partial u}{\partial y}\right) \tag{10}$$

Here, i,j,k represent the directional coordinates in the x,y,z directions, respectively; $\Delta x_i$, $\Delta y_j$, $\Delta z_k$ represent the coordinate width immediately following those coordinates designators, and tabulate as $u^i_jk = u(x_i, y_j, z_k)$. The difference operators $\delta_y$ and $\Delta_y$ are formulated, respectively as follows: /212

$$\delta_y u^i_{jk} = \frac{(\Delta y_{j-1})^2(u^i_{j+1k} - u^i_{jk}) + (\Delta y_j)^2(u^i_{jk} - u^i_{j-1k})}{\Delta y_{j-1}\Delta y_j(\Delta y_{j-1} + \Delta y_j)} \tag{11}$$

$$\Delta_y(\nu^i_{jk}\Delta_y u^i_{jk}) = \frac{2}{\Delta y_{j-1} + \Delta y_j}\left\{\nu^i_{j+\frac{1}{2}k}\frac{u^i_{j+1k} - u^i_{jk}}{\Delta y_j} - \nu^i_{j-\frac{1}{2}k}\frac{u^i_{jk} - u^i_{j-1k}}{\Delta y_{j-1}}\right. \tag{12a}$$

$$\nu^i_{j\pm\frac{1}{2}k} = \frac{1}{2}(\nu^i_{jk} + \nu^i_{j\pm 1k}) \tag{12b}$$

The difference operator $\delta_z$ attempts to become equation (11). At this time, the PC-CN scheme is a two-stage semi-implicit scheme which can be expressed as follows (Figure 3, scheme (f)):
predicator:

$$u^i_{jk}\frac{\overline{u^{i+\frac{1}{2}}_{jk}} - u^i_{jk}}{\Delta x_i/2} + func(x_{i+\frac{1}{2}}, z_k, u^i_{jk}, \delta_z u^i_{jk}, \delta_y u^i_{jk}) = \Delta_y(\nu^i_{jk}\Delta_y \overline{u^{i+\frac{1}{2}}_{jk}}) \tag{13}$$

Corrector:

$$\overline{u^{i+\frac{1}{2}}_{jk}}\frac{u^{i+1}_{jk} - u^i_{jk}}{\Delta x_i} + func(x_{i+\frac{1}{2}}, z_k, \overline{u^{i+\frac{1}{2}}_{jk}}, \delta_z \overline{u^{i+\frac{1}{2}}_{jk}}, \delta_y \overline{u^{i+\frac{1}{2}}_{jk}}) = \frac{1}{2}\left\{\Delta_y(\overline{\nu^{i+\frac{1}{2}}_{jk}}\Delta_y u^{i+1}_{jk}) + \Delta_y(\overline{\nu^{i+\frac{1}{2}}_{jk}}\Delta_y u^i_{jk})\right\} \tag{14}$$

/211

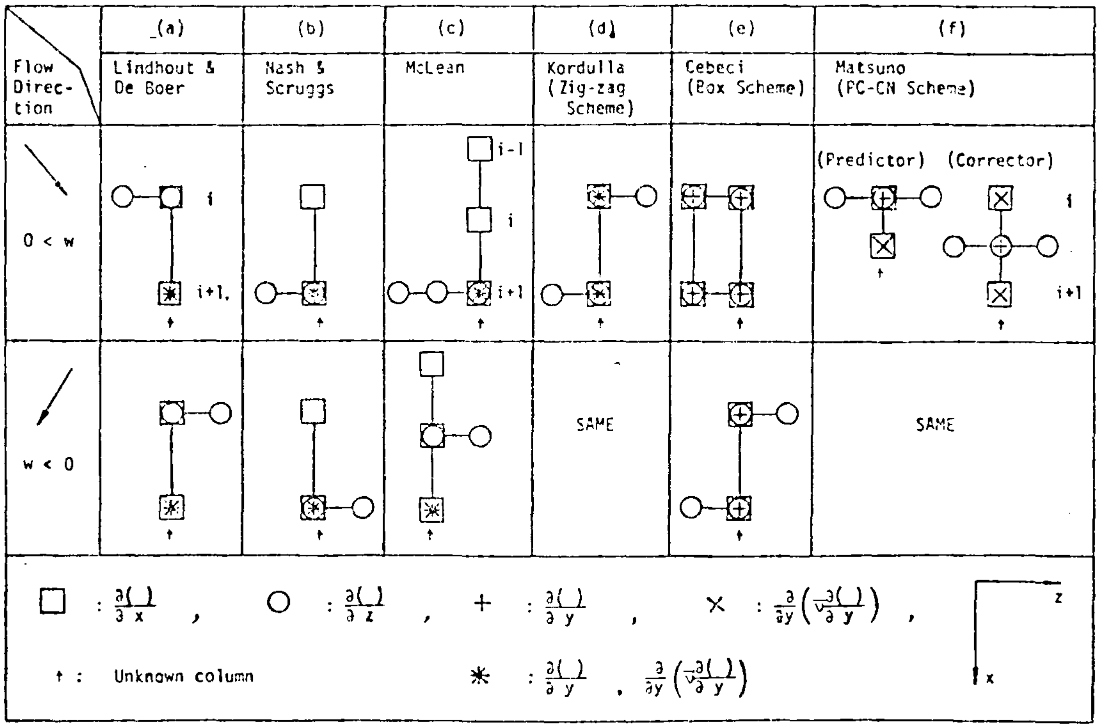


Figure 3. Difference schemes applied to three-dimensional boundary layer equation

This scheme is characterized as follows: (1) It is linear with respect to unknown quantities (predictor step is $u^{i+1/2}$; corrector step is $u^{i+1}$). All calculations are accomplished in two stages--predictor and corrector--with no iterative process. Therefore, as a whole, the computer operation load per coordinate point is low and the system is efficient; (2) since the z differential term is expressed in a three-point difference core, the scheme itself depends on the w code and does not change; (3) as to the unknown quantity, it is implicit in the j direction, but explicit in the k direction and mutually independent. Therefore, in the k direction array, parallel processing becomes possible; (4) the /212
accuracy in the z direction is second order for $\Delta z$; (5) evaluation

of the turbulent vortex viscosity can be performed directly at 1 + 1/2 without iteration, thus facilitating the introduction of various high order turbulent models. Furthermore, it allows for consideration only of the CFL condition ($\Delta x/\Delta z$ less than u/w) on the x-y plane, as the stability condition for the scheme in the case of boundary layer equation in a manner similar to ther implicit schemes.

### 2.3 Features of the BLAY

Compared with other existing programs the BLAY possesses the following features:

(1) the required computing time is the shortest

(2) it is suitable for parallel processing computers

(3) it has a second order accuracy in the z direction, too.

As to item (1) above, there is no iterative convergence process in the respective steps; and the linearization of the ion linear terms can be traced to the fact that the process is simple and the operation load is low. We will next express this specifically with the example of the nonlinear term $u(\partial u/\partial x)$ . If, as a typical example of other high efficiency difference methods we cite the scheme that iteratively linearizes the second order accurate Newton Raphson model, it will be differentiated as follows (subscripts jk omitted)

$$u\frac{\partial u}{\partial x} \rightarrow \frac{1}{2}(u^{i+1}+u^{i})\cdot\frac{1}{\Delta x_i}(u^{i+1}-u^{i}) \qquad (15)$$

$$\rightarrow \frac{1}{2\Delta x_i}\cdot\left\{\tilde{u}^{i+1}\cdot(2\tilde{u}^{i+1}-u^{i+1})-(u^{i})^{2}\right\}$$

Here $\tilde{u}^{i+1}$ will be established as the initial estimated value or the pre-iteration value. We think of multiplication as a necessary operation load. If we assume the number of iterative cycles as the minimum 2, equation (15) becomes, for each coordinate point

multiplication load $\geq$2 x (iterative calculation: 3 cycles) +1 = 7(cycles) (16)

Even when we consider Cebeci's Box scheme, which is known as another high efficiency difference method and anticipating a minimum operation cycle load by aggressively conserving an intermediate calculated value, we obtain a value the same as equation (16). On the other hand, for the BLAY PC-CN scheme, as indicated by equations (3) and (14), they become

(predictor):

$$u\frac{\partial \dot{u}}{\partial x} \rightarrow u^{i}\cdot\frac{2}{\Delta x_i}\cdot\left(\overline{u^{i+\frac{1}{2}}}-u^{i}\right) \tag{17a}$$

(corrector): /21

$$u\frac{\partial u}{\partial x} \rightarrow \overline{u^{i+\frac{1}{2}}}\cdot\frac{1}{\Delta x_i}\cdot\left(u^{i+1}-u^{i}\right) \tag{17b}$$

Therefore, the number of multiplications for each coordinate point becomes:

$$\text{multiplication load} = 2 + 2 = 4 \text{ (cycles)} \tag{18}$$

Let us now make a comparison using the actually measured value of the required computing time. To assure fairness, let us take the input/output portion of the BLAY without change and discuss the results of the numerical experiment conducted by replacing only the difference scheme. Taking as an example the problem of a tapered, backward swept wing configuration with coordinate grid numbers l x j x k x 2 (upper and lower wing surfaces) equal to 40 x 35 (average) x 41 x 2, and utilizing the FACOM M380 general purpose computer, the required computer time (excluding input/output) was 25 seconds for the linearized Newton Raphson model integrated into the Krause zigzag implicit scheme; and 10 seconds for the PC-CN scheme.

## 4. Examples of application computation

In order to conduct a computation, it is necessary as a boundary condition on the outer fringe of the boundary layer for the value of nonviscous flow to be given in terms of velocity components. The calculation results described below are derived, using nonviscous flow data on the outer fringe of the boundary layer as follows:

in the case of the low velocity incompressible flow problem, the results from the panel method; and for all other cases, the calculation results from applying the transonic total potential flow analysis program (AFPWING) [14]. Here under the pressure gradient of the given boundary layer outer fringe the focus is on the feasibility of the BLAY being indicated as well as to denote what type of three-dimensional boundary layer flow is formed on the wing surface under that type of pressure distribution. Nonviscous-viscous interference is important, but is a separate problem, hence, will not be addressed here.

Firstly, the results of computation in response to Brebner and Wyatt's experience [15] which was conducted for the purpose of investigating the validity of the BLAY boundary layer computation method are shown in Figure 4. In the figure, comparison is made only at one point but it is about the same even when several points are investigated. From this figure, it can also be seen for the boundary layer internal specific value that at the present time, even though many unsolved problems are yet encountered, it will be necessary to take into account viscous/nonviscous interference. Further, it will be necessary to investigate the turbulent flow model.

Next, we show a calculation sample from the transonic flow problem. Generally, as a characteristic of transonic flow, in the reverse pressure gradient region, where the shock wave effect is strong even though localized, the boundary layer there peels off and /214 the capability to calculate thereafter becomes ineffective. Since the BLAY scheme by virtue of its purpose prioritizes on the calculation over the flow field in entirety, it has incorporated the FLARE [16] approximation which permits approximate calculation of small separation regions. This approximation is based on an estimate that the convection term ($u\partial(\ )/\partial x$) within the reverse flow region is zero. Therefore, for a small, localized separation region it is known that a significant effort is not generated. However, in reality, there are many cases where computation can be performed without

/213

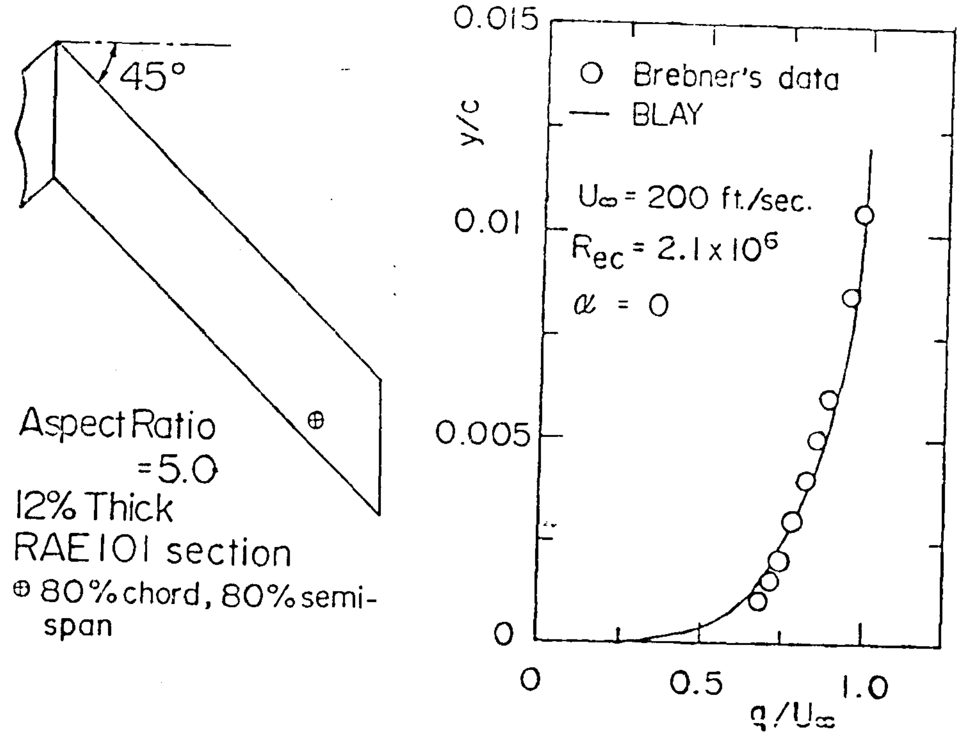


Figure 4. Comparison of computed value and experimental value

/214

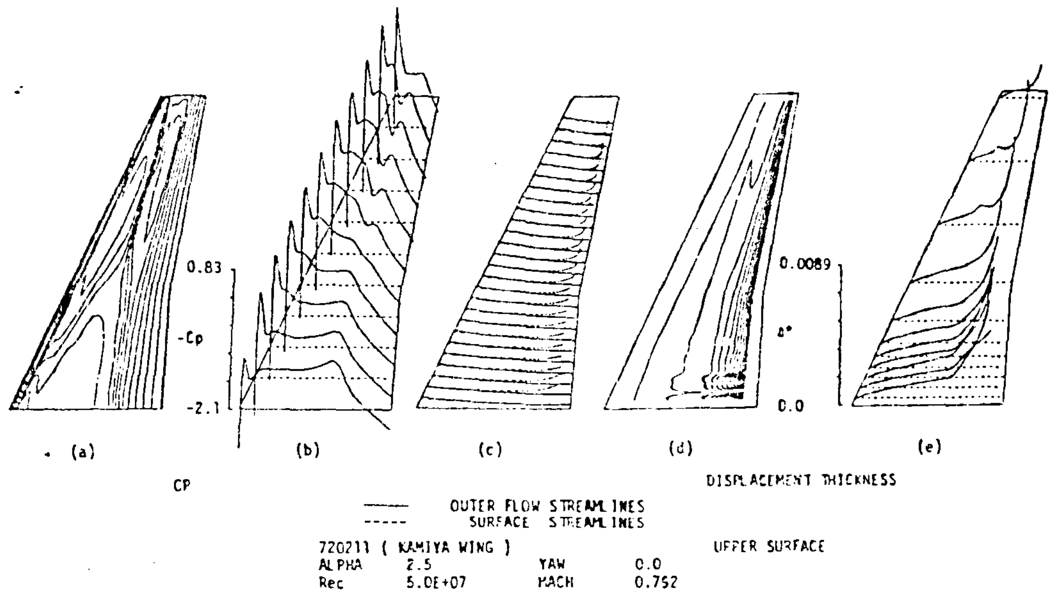


Figure 5. Pressure distribution and boundary layer for the 720211 wing (wing upper surface)

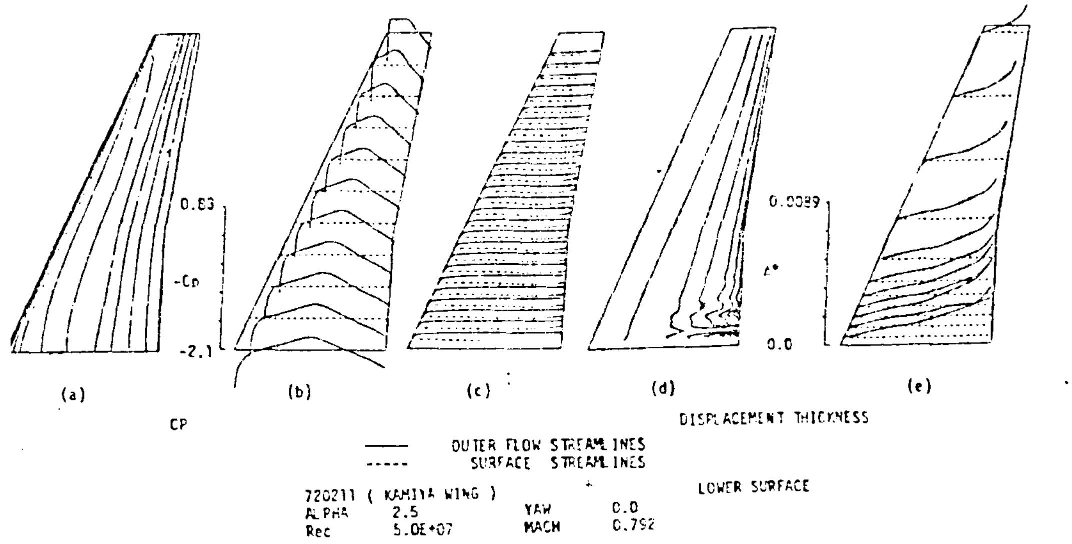


Figure 6. Pressure distribution and boundary layer for the 720211 wing (wing lower surface)

incorporating a FLARE approximation by the fact that the shock wave itself is weakened numerically, and in the fact of applying turbulent flow of high Reynold's number. Results from four types of cases are shown below. Figures 5 through 9 show the results, graphically, of five sets of five plots which are from left to right: (a) pressure contours, (b) pressure distribution, (c) comparative plots of the body surface streamlines (limiting streamlines and broken lines) of the boundary layer outer fringe streamlines (continuous lines) and boundary layer, (d) boundary layer displacement thickness ($\Delta^*$) contours, (e) boundary layer displacement thickness distribution. The flow direction in all figures is from left to right. The terms in the figures are defined as follows: ALPHA: angle of attack; Re: /215
Reynold's number; MACH: Mach number; YAW: yaw angle. Calculations were conducted for the four cases discussed below. We assume that the flow field is turbulent in practically all regions, and that laminar flow transitions to turbulent flow at x = 1% chord.

Firstly, the computation results on the transonic wing (Kamiya 720211 wing [14]) are shown in Figure 5 (upper surface of wing) and

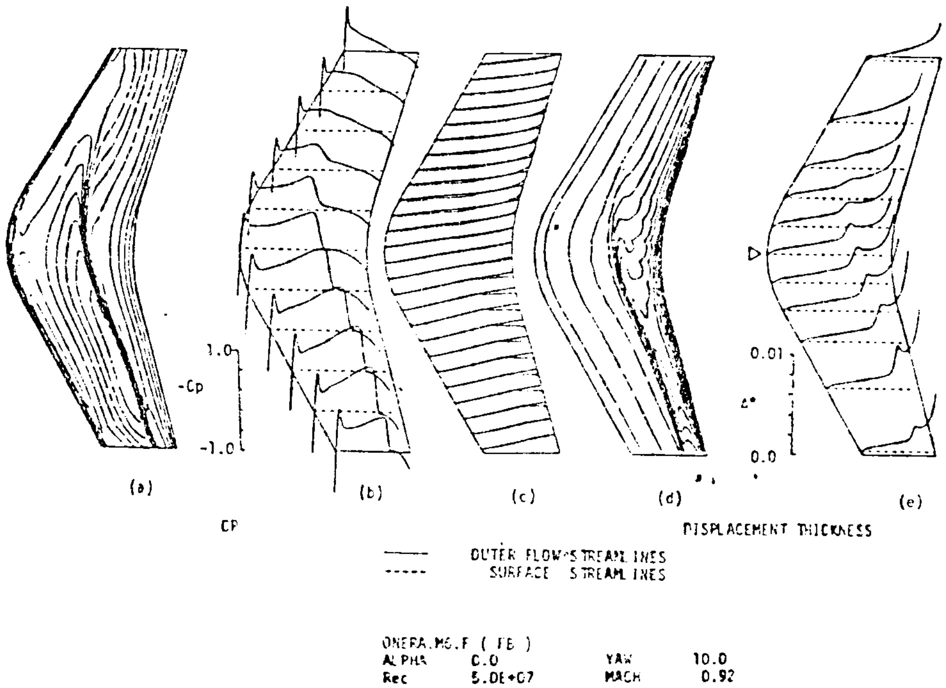


Figure 7. Pressure distribution and boundary layer over isolated swept back wings.

Figure 6 (lower surface of wing). The main stream Mach number is 0.792; and the principal feature of the pressure distribution is that a strong shock wave exists on the upper wing surface's outer wing, and a pressure flattening exists in the vicinity of the wing root area. On the wing lower surface, the flow is subsonic over the entire region. The coefficient of lift, $C_L$, for this case is 0.566. We will first discuss the results of the boundary layer calculation along the wing upper surface. The calculation encounters the first reverse flow region (peeling off at the trailing edge) at 73% semi-span and 82% chord position, and the calculation continues thereafter to 86% chord by means of the FLARE approximation. However, since the separation region is large, the calculation thereafter becomes impossible. A special feature of the boundary layer that can be cited is that as seen in Figure 5(d) a region of extremely strong three-dimensional characteristics appears in the wing root area. This type of region can also be observed in the calculation results of McLean's Boeing transport aircraft transonic wing. This region does not appear even in the case, for example, of calculation over

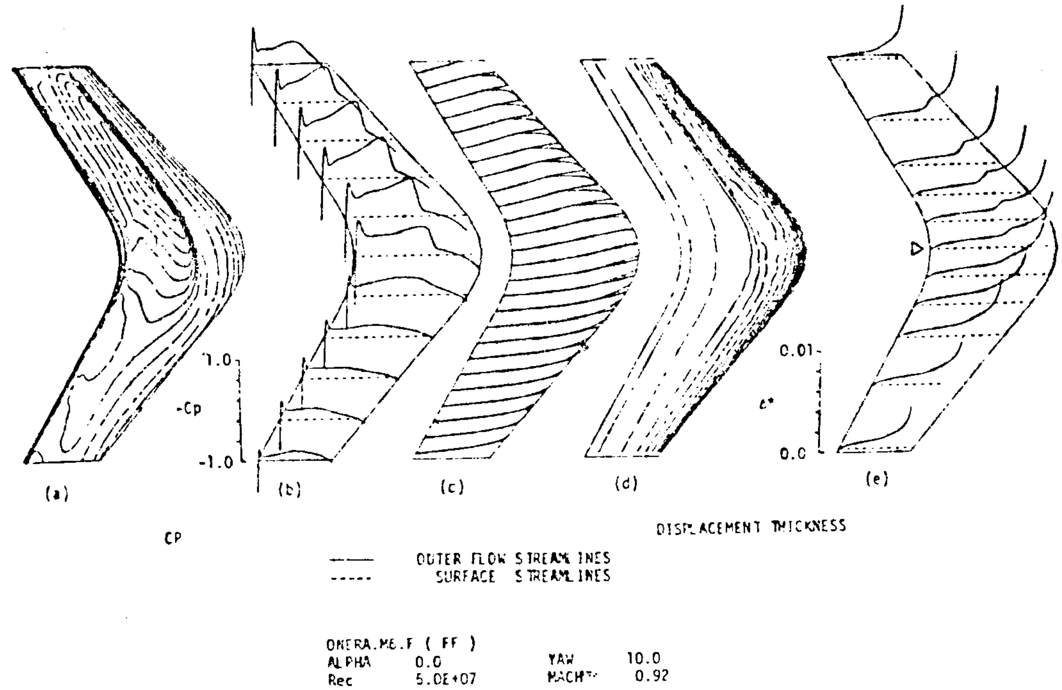


Figure 8. Pressure distribution and boundary layer over isolated forward swept wings.

/216

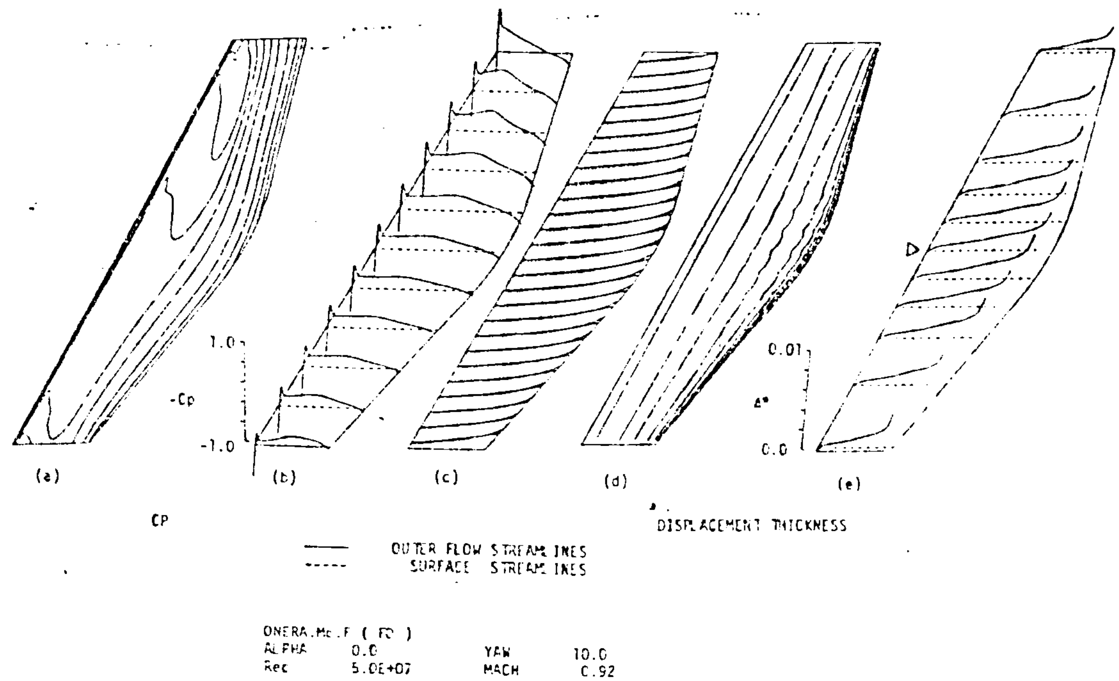


Figure 9. Pressure distribution and boundary layer over isolated oblique wings.

a wing configured in a flat surface space distribution the same as for the 720211 wing with a NACA 0012 wing profile [17]. We will next discuss the lower surface of the wing (Figure 6). The calculation is performed to the trailing edge. The principal feature of the boundary layer is again that a region with a strong three-dimensional character is indicated in the wing root area. In the outer wing contours of displacement thickness appear parallel to the leading edge, and two-dimensionally except at the trailing edge area. /215

Next, let us consider three cases of independent wings (backward swept, forward swept and oblique) having a yaw angle in the flow field, and perform a comparative investigation of their boundary layers. Analyzed are planar configurations as shown in Figures 7 through 9, whose cross sectional profiles are similar to the ONERA M6. The three types of wing planar configurations are compared against a baseline configuration which provides a complete match in terms of the aspect ratio, the leading edge sweep back angle (±30°), and the chord length at various span stations. Conditions are: Mainstream Mach number, 0.92; angle of attack, 0°; yaw angle, 10°. First, let us compare the characteristics of the external nonviscous flow (Figures 7 through 9(a),(b), (c)). The swept back wing acquires an additional yaw angle, resulting in a high, effective Mach number--in the case of the swept back wing (Figure 7), on the left side; and in the case of the forward swept wing, on the right side. As a great difference in the respective pressure distributions, we can cite the existence of non-existence of a shock wave at the wing tip areas. The existence of a strong shock wave can be acknowledged for the swept back wing; but for the forward swept wing the status is "no shock wave". For the oblique wing, because of the yaw angle, /217
an additional 10° sweep back develops at the leading edge. As a result, the effective Mach number is low, and the condition over the entire wing area is "no shock wave". The boundary layers under these pressure distributions are shown in Figures 7 through 9(c),(d) and (e). First, considering the boundary layer surface streamlines, what is unique is that the flow (frictional resistance) for the swept

back wing is in the direction of the wing's external side and for the forward swept wing, in the direction of the wing's internal side. At the same time, the surface streamlines turn substantially at the point where the shock wave exists. On the other hand, in the case of the oblique wing, the surface streamlines in their entirely flow in the direction of the right wing tip which corresponds to the downstream side. Next, comparing the boundary layer according to the displacement thickness in the case of the swept back wing, the displacement thickness is greatly increased at the shock wave position as can be seen in Figure 7(d) and (e), and the contour lines become more dense.

On the other hand, if we consider the same aspect for the forward swept wing, it is seen from Figure 8(d) that the increase in the displacement thickness at the shock wave position is not as great as in the case of the swept back wing. If we consider the boundary layer in entirety, the displacement thickness distribution of the forward swept wing can be said, as shown in Figure 8(d) to have its contours run in parallel with % chord in practically all regions, and two-dimensional. For the same aspect, in the case of the oblique wing, it is even more two-dimensional (Figure 9(d)). Shown in Figure 10 is a comparison of the distribution of displacement thickness at the central 50% span position (denoted by ▷ in Figures 7 through 9(e)) for the purpose of comparing the conditions surrounding the development of the boundary layer. Up to the 30% chord point, the boundary layer development is about the same for the swept back and forward swept wings; but beyond that and up to 55% chord, the displacement thickness increase is greater for the swept back wing. The rapid increase of the displacement thickness at the shock wave position is more rapid in the case of the swept back wing than with the forward swept wing proportionally to the strength of the shock wave. On the other hand, the increase of the displacement thickness in the case of the oblique wing is monotonic as a whole, and merely increases abruptly in the trailing edge area. If we estimate the displacement thickness as a viscous effect, we see that the displacement thickness

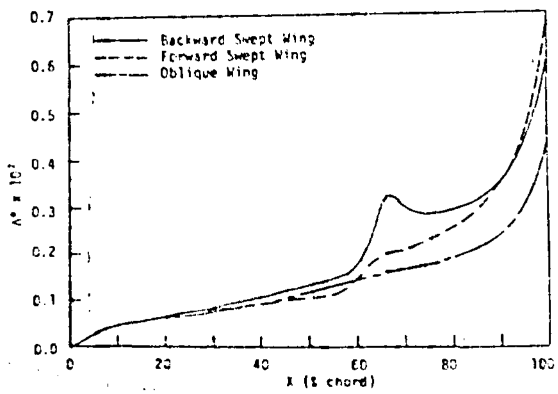


Figure 10. Comparison of displacement thickness at the central areas of swept-back, forward swept and oblique wings.

increase is greatest for the oblique then the forward swept and swept back wings, in that order.

## 5.. Conclusions

In this paper, we emphasized the BLAY's high efficiency of the boundary layer analysis program as an aerodynamic design tool for the viscous and nonviscous weak interference problem(s) as a boundary layer correction in particular, to the transonic nonviscous flow analysis program, we find that it can be repeatedly used several tens of times. Therefore, its high efficiency is a most important element from cost considerations.

The BLAY is a code developed from a baseline research code developed in 1980 by one of the authors whereby the input/output segment was generalized and a compensatory function added to the computing segment to achieve a pilot code, and then a production code. The BLAY is being applied to various flow problems, thus allowing for experience to be accumulated in its application scope, robustness, reliability, etc. What is introduced in this paper includes one portion (of that experience), but it can be said that for the calculation of boundary layers, they have in all cases been performed under rigorous conditions. It is believed that this program rates high in its reliability because of the simplicity of the scheme and its algorithms.

We express our gratitude for the fact that Ms.Michiko Kikuchi of Fujitsu Incorporated (Kabushiki Kaisha) bore a large portion of the generalization work in the development of the BLAY. Mr. Kohei Suetsugu also of Fujitsu provided his good offices to expedite the use of the "AFPWING" program. We express our deepest thanks.

/217

## REFERENCES
/218


1) Nash, J. F. and Scruggs, R. M. (1972) NASA CR-112158

2) Nash, J. F. and Scruggs, R. M. (1978) Lockheed Report LG78ER0241

3) Cebeci, T., Kaups, K. and Ramsey, J. A. (1977) NASA CR-2777

4) McLean, J. D. (1977) AIAA Paper 77-3

5) McLean, J. D. and Randall, J. L. (1978) NASA CR-3123

6) Bradshaw, P., Mizner, G. A. and Unsworth, K. (1975) Aero Rept. 75-04, Imperial College, London

7) Lindhout, J. P. F. and DeBoer, E. (1976) NLR TR 76086U

8) Lindhout, J. P. F., Moek, G., DeBoer, E. and Van den Verg, B. (1979) Turbulent Boundary Layers, ASME

9) Kordulla, W. (1977) AIAA Paper 77-209

10) Rostogi, A. K. and Rodi, W. (1979) Turbulent Boundary Layers, ASME

11) Matsuno, Ken-ichi: (1979) 17th Aviation Symposium (Hikoki Shinpojimu) Papers (Ronbunshu)

12) Matsuno, Ken-ichi: (1980) 18th Aviation Symposium Papers

13) Matsuno, K. (1981) AIAA Paper 81-1020, 5th CFD Conf. AIAA

14) Ishiguro, Tomiko: (1982) NAL TR-731

15) Brebner, G. G. and Wyatt, L. A. (1961) NRC CP.No. 554

16) Bradshaw, P., Cebeci, T. and Whitelaw, J. H. (1981). Engineering Calculation Methods for Turbulent Flow, Academic Press

17) Matsuno, Ken-ichi, et al.: NAL TR Publication projected.